Received: 14 September 2023 | Revised: 6 November 2023 | Accepted: 9 November 2023

DOI: 10.1002/mrc.5417

RESEARCH ARTICLE

WILEY

Polarization transfer methods for quantitative analysis of flowing mixtures with benchtop ^{13}C NMR spectroscopy

Johnnie Phuong[1,2] | **Zeno Romero**[1,2] | **Hans Hasse**[1,2] | **Kerstin Münnemann**[1,2]

[1]Laboratory of Engineering Thermodynamics (LTD), RPTU Kaiserslautern, Kaiserslautern, Germany

[2]Laboratory of Advanced Spin Engineering - Magnetic Resonance (LASE-MR), RPTU Kaiserslautern, Kaiserslautern, Germany

Correspondence
Kerstin Münnemann, Laboratory of Engineering Thermodynamics (LTD), RPTU Kaiserslautern, Erwin-Schrödinger-Straße 44, 67663 Kaiserslautern, Germany.
Email: kerstin.muennemann@rptu.de

Funding information
German Research Foundation (DFG), Grant/Award Number: CRC 1527 HyPERiON

Abstract

Benchtop NMR spectroscopy is attractive for process monitoring; however, there are still drawbacks that often hamper its use, namely, the comparatively low spectral resolution in ^{1}H NMR, as well as the low signal intensities and problems with the premagnetization of flowing samples in ^{13}C NMR. We show here that all these problems can be overcome by using ^{1}H-^{13}C polarization transfer methods. Two ternary test mixtures (one with overlapping peaks in the ^{1}H NMR spectrum and one with well-separated peaks, which was used as a reference) were studied with a 1 T benchtop NMR spectrometer using the polarization transfer sequence PENDANT (polarization enhancement that is nurtured during attached nucleus testing). The mixtures were analyzed quantitatively in stationary as well as in flow experiments by PENDANT enhanced ^{13}C NMR experiments, and the results were compared with those from the gravimetric sample preparation and from standard ^{1}H and ^{13}C NMR spectroscopy. Furthermore, as a proxy for a process monitoring application, continuous dilution experiments were carried out, and the composition of the mixture was monitored in a flow setup by ^{13}C NMR benchtop spectroscopy with PENDANT. The results demonstrate the high potential of polarization transfer methods for applications in quantitative process analysis with benchtop NMR instruments, in particular with flowing samples.

KEYWORDS

^{1}H; ^{13}C, benchtop NMR, flow NMR, polarization transfer, process monitoring, quantitative analysis

1 | INTRODUCTION

Process analytical technologies (PAT) are essential for the effective control, operation and optimization of chemical and/or biological process.[1] Nuclear magnetic resonance (NMR) spectroscopy is a powerful tool for process and reaction monitoring applications due to several advantages over other established methods such as gas chromatography, infrared, and mass spectroscopy[2–8]: NMR allows a noninvasive elucidation of the composition, an external calibration is not required, and the

Dedicated to our colleague and friend Michael Maiwald, who passed away much too soon.

method is capable of continuous flow analysis in bypass setups. The advent of benchtop NMR spectrometers has made NMR spectroscopy an even more attractive PAT tool.[9–17] Instead of using superconducting magnets that must be cooled by cryogenic media, benchtop NMR spectrometers are equipped with permanent magnets. The spectrometers are therefore compact, comparatively inexpensive to purchase and to maintain, and easy to operate. Benchtop NMR spectrometers have already been used in research to monitor a variety of reactions and processes, highlighting the promising prospects for future use in industrial applications.[18–29]

However, the relatively low magnetic field strength of benchtop NMR spectrometers results in low spectral resolution, even at field strengths of up to 2.5 T that have become available recently. The resulting peak overlap, especially in combination with peak splitting, impedes the quantitative analysis of mixtures by ^{1}H NMR spectroscopy. The problems become even worse in flow experiments where peak broadening occurs which is caused by the reduction of the spin–spin relaxation time T_2^* due to outflow-effects.[3,10]

Peak deconvolution methods such as CRAFT (Complete Reduction To Amplitude Frequency Table), IHM (Indirect Hard Modeling), and GSD (Global Spectrum Deconvolution) or the Bayesian method introduced recently by Matviychuck et al.[30–33] can be used to tackle the peak overlap issue. However, all these methods have limitations and become unreliable if the peaks overlap too strongly. Their application also introduces further uncertainty in the quantification and generally requires expert knowledge.

Another approach to improve the spectral resolution is to use 2D NMR experiments. The measurement time of 2D NMR experiments, which is usually long, can be reduced by ultrafast 2D acquisition schemes.[34,35] However, the implementation and application of these complex pulse sequences require expert knowledge as well as spectrometers that are equipped with gradient systems.

The seemingly most simple way to tackle the peak overlap problem is to switch from ^{1}H NMR to ^{13}C NMR.[36–38] Peak overlap problems are rare in ^{13}C NMR spectroscopy, due to the higher chemical shift dispersion of ^{13}C compared with ^{1}H. Moreover, ^{1}H decoupling sequences can be used to avoid peak splitting. However, this big advantage of ^{13}C NMR comes at the cost of a much poorer signal-to-noise ratio (SNR) compared with ^{1}H NMR, caused by the low natural abundance of ^{13}C nuclei and their low gyromagnetic ratio. This is particularly detrimental for benchtop NMR spectrometers because of their low magnetic field strength and often results in extremely long measurement times needed to obtain useful ^{13}C NMR spectra. In addition, ^{13}C nuclei have a long magnetization build-up time in flow applications due to the long spin–lattice relaxation time $T_{1,^{13}C}$, which is several times higher than that of ^{1}H nuclei. This causes problems with the premagnetization of flowing samples, which are worsened by the fact that the premagnetization volumes in benchtop instruments are low, due to their compact design.[2,39] The premagnetization problem can be tackled with paramagnetic relaxation agents which, however, complicate the measurement.[40] Furthermore, for routine measurements in industry, the agents must meet high stability requirements, and the technique is still far from being routine.

The application of polarization transfer pulse sequences can solve all problems mentioned above: They provide a fourfold signal enhancement of the ^{13}C signal via polarization transfer from scalarly coupled ^{1}H spins. In addition, the repetition delay between successive scans can be reduced, since the much shorter spin–lattice relaxation time $T_{1,^{1}H}$ of ^{1}H nuclei is used for magnetization build-up, which also substantially lessens the problems with flowing samples. This combination of advantages of polarization transfer pulse sequences makes them highly attractive for process monitoring applications with benchtop NMR.

Commonly used polarization transfer pulse sequences are INEPT and DEPT.[41–43] However, these sequences cannot detect quaternary carbon atoms, that is, the corresponding information is lost. The lesser known polarization transfer sequence PENDANT (abbreviation for polarization enhancement that is nurtured during attached nucleus testing) of Homer and Perry[44,45] combines several advantages: enhancement of ^{13}C signals to which ^{1}H atoms are bound, selective excitation of functional carbon groups (CH_3, CH_2, and CH) and detection of quaternary carbon atoms. To the best of our knowledge, polarization transfer techniques have not been used before for quantitative process monitoring with benchtop NMR spectroscopy, particularly not for flowing samples.

To demonstrate the feasibility of using polarization transfer techniques for the quantitative analysis of mixtures with benchtop NMR, we have carried out experiments with two test mixtures using the polarization transfer sequence PENDANT. The mixtures were analyzed quantitatively in stationary and flow experiments. The results obtained with the polarization transfer sequence PENDANT were compared with the gravimetrically determined concentrations and results from standard ^{1}H and ^{13}C NMR analysis. Furthermore, a continuous dilution experiment was carried out that is considered here as a proxy of a dynamic process, and the ^{13}C NMR PENDANT technique was applied for its monitoring.

2 | EXPERIMENTAL SECTION

2.1 | Chemicals and sample preparation

The chemicals used in this work are summarized in the Supporting Information. They were used without further purification. Two test systems were investigated:

- System 1: acetonitrile (ACN) + dimethyl sulfoxide (DMSO) + ethyl formate (EF), in which all peaks are well-separated in the ^{1}H NMR spectrum.
- System 2: acetonitrile (ACN) + acetone (ACT) + ethyl formate (EF), in which peaks overlap in the ^{1}H NMR spectrum.

Mixtures of different compositions were prepared gravimetrically with a laboratory balance (Delta Range XS603S, Mettler Toledo) with an accuracy of ±0.001 g; Table 1 gives an overview.

2.2 | NMR hardware and experiments

All experiments were carried out with a benchtop NMR spectrometer from Magritek (Spinsolve Carbon) with a magnetic field strength of $B_0 = 1$ T corresponding to a ^{1}H Larmor frequency of $\nu_0 = 42.5$ MHz. The polarization transfer pulse sequence PENDANT for the signal enhancement in the ^{13}C NMR spectrum was implemented on the benchtop NMR spectrometer with the software Spinsolve Expert (Magritek). The evolution delays as well as the phase cycle were adopted as published by Homer & Perry.[44,45] An inverse-gated decoupling sequence (WALTZ-16) for ^{1}H decoupling during the acquisition of the FID is included. The experiment is referred to as ^{13}C NMR PENDANT in the following and is illustrated in the Supporting Information. The evolution delays of the pulse sequence are given in the Supporting Information. Depending on the setting for the scalar coupling constant $^1J_{C,H}$ between the carbon and the scalarly coupled proton, either the signal of CH_3-, CH_2-, or CH-group is fully enhanced. In this work, the $^1J_{C,H}$ was set to fully enhance the CH_3-group of each molecule.

2.2.1 | Stationary experiments

The stationary experiments were executed in NMR sample tubes with an outer diameter of $d = 5$ mm (Magritek). The spin–lattice relaxation times $T_{1,^1H}$ and $T_{1,^{13}C}$ were determined with the inversion recovery experiment from the standard operating software of the spectrometer.

The quantitative analysis of the mixtures was performed using a ^{1}H NMR, ^{13}C NMR, and the ^{13}C NMR PENDANT experiment controlled by the Spinsolve Expert software. ^{1}H NMR experiments were executed with an acquisition time of 6.4 s, 32 k data points, four scans, and a 90° excitation pulse. The parameters for the ^{13}C NMR as well as the ^{13}C NMR PENDANT experiment were 3.2 s acquisition time, 16 k data points, and 128 scans. For the ^{13}C NMR experiments, a 90° excitation pulse and a WALTZ-16 decoupling sequence during the acquisition were applied. The repetition time in all experiments was set to guarantee a sufficient magnetization recovery of the sample with at least five times T_1.

All spectra were postprocessed with the automatic baseline and phase correction tool SINC.[46,47] The determination of the SNR as well as the integration of the peaks for the quantitative analysis were performed in MestRenova. The overlapping peaks in the ^{1}H NMR spectrum in System 2 were analyzed with the Global Spectral Deconvolution (GSD) tool included in MestRenova. The mole fraction of a component in the ternary mixtures was determined by the normalized peak integral fraction of that component with respect to all components in the mixture. For the quantitative analysis only the signal of the CH_3-group of each component was considered. The uncertainties of the results for the mole

TABLE 1 Overview of the studied mixtures.

System 1: ACN + DMSO + EF				System 2: ACN + ACT + EF			
	x_{ACN}	x_{DMSO}	x_{EF}		x_{ACN}	x_{ACT}	x_{EF}
Mixture	mol mol^{-1}			Mixture	mol mol^{-1}		
1.A	0.333	0.333	0.334	2.A	0.333	0.333	0.334
1.B	0.700	0.150	0.150	2.B	0.700	0.150	0.150
1.C	0.150	0.700	0.150	2.C	0.150	0.700	0.150
1.D	0.150	0.150	0.700	2.D	0.150	0.150	0.700

fractions that are reported here were determined from the uncertainty of the peak areas as described in the Supporting Information. For evaluating the ^{13}C NMR PENDANT experiment, the relative deviation ($\Delta_{i,rel}$), the root mean squared error (RMSE), and the mean absolute error (MAE) are used:

$$\Delta_{i,\mathrm{rel}} = \left(\frac{x_{i,\mathrm{method}} - x_{i,\mathrm{reference}}}{x_{i,\mathrm{reference}}}\right) 100\% \quad (1)$$

$$\mathrm{RMSE} = \sqrt{\frac{\sum_{i=1}^{N} \left(x_{i,\mathrm{method}} - x_{i,\mathrm{reference}}\right)^2}{N}} \quad (2)$$

$$\mathrm{MAE} = \frac{\sum_{i=1}^{N} \left|x_{i,\mathrm{method}} - x_{i,\mathrm{reference}}\right|}{N} \quad (3)$$

Here, i denotes the component, N the total number of concentrations determined by that method, and x_i the mole fraction of component i. Calculating the MAE and RMSE as error scores is a common practice in data science. While MAE provides a measure of the absolute error between the method and the reference, RMSE penalizes large errors more strongly, thus highlighting the impact of outliers. A direct comparison of MAE and RMSE provides insight into the underlying error distribution. If the RMSE is much higher than the MAE, the score is usually strongly influenced by outliers.

2.2.2 | Flow experiments

Figure 1 shows the closed loop setup used for the flow experiments. The liquid feed mixture was stored in a $V = 100$ mL feed container. A double piston high-pressure pump with damping piston (WADose LITE HP, Flusys) was used to circulate the sample. The flow rate was measured with an accuracy of ±2 % with a Coriolis sensor (Mini Cori-Flow, Bronkhorst) that was also used to control the pump. The mixture was transported through PEEK capillaries with an inner diameter of $d = 1$ mm to the benchtop NMR spectrometer that was equipped with a glass flow cell (Spinsolve Reaction Monitoring Kit RM, Magritek). The flow cell has an inner diameter of $d = 1$ mm at the inlet and the outlet; in the active region, the diameter is $d = 4$ mm.

Flow rates in the range of $\dot{V} = 0.5$ to 2 mL min^{-1} were set in 0.25 mL min^{-1} steps. These flow rates correspond to the following flow velocities: capillaries (1–4 cm s^{-1}); detection volume (0.1–0.3 cm s^{-1}). For the quantitative analysis of the flowing sample, ^1H NMR, ^{13}C NMR, and ^{13}C NMR, PENDANT experiments were performed with the same parameters as in the stationary experiments. ^{13}C NMR and ^{13}C NMR PENDANT experiments were executed with 64 scans. The accumulation of multiple scans was performed with a delay time t_d which depends on the investigated mixture as well as on the observed nucleus and was set according to Equation (4)[3,10]:

$$t_d = \frac{1}{\frac{1}{T_1} + \frac{1}{t_{DV}}} \quad (4)$$

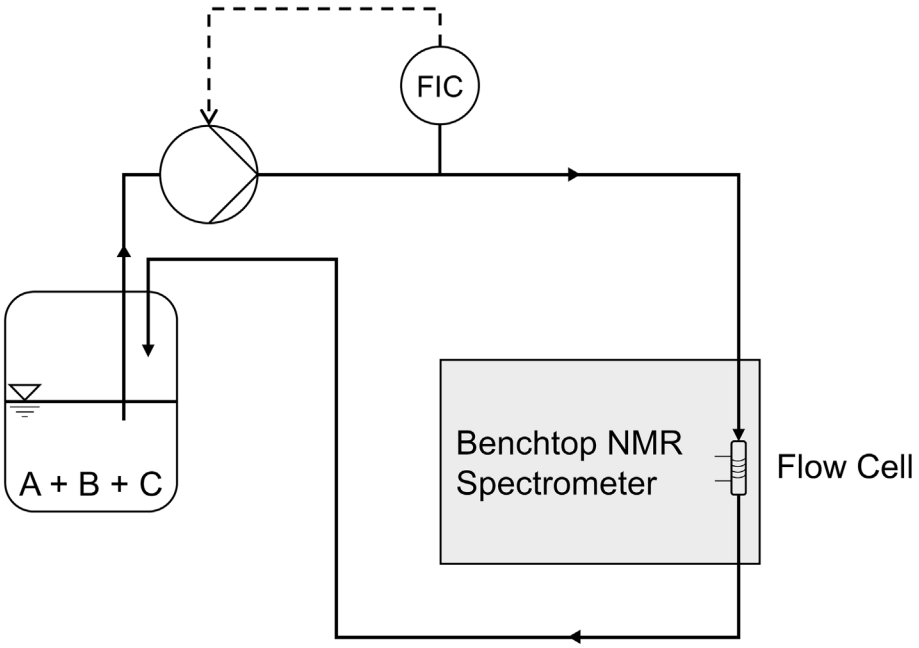

FIGURE 1 Scheme of the setup used for flow experiments.

Here, T_1 is the longest spin–lattice relaxation time of the mixture and t_{DV} the residence time of the spins inside the detection volume, which depends on the adjusted flow rate. An additional safety margin of 2 s was added to the delay time t_d calculated from Equation (4), to ensure a full replenishment of nonexcited spins. The postprocessing steps as well as the quantitative analysis were performed as in the stationary experiments (see Section 2.2.1).

2.2.3 | Process monitoring experiments

Figure 2 depicts the setup used for the process monitoring experiments, in which a continuous dilution process was monitored. The setup of flow experiments (see Figure 1) was adopted and extended by an additional feed container with a total volume of $V = 100$ mL as well as a second double piston high-pressure pump with damping piston (WADose PLUS HP, Flusys). A binary mixture

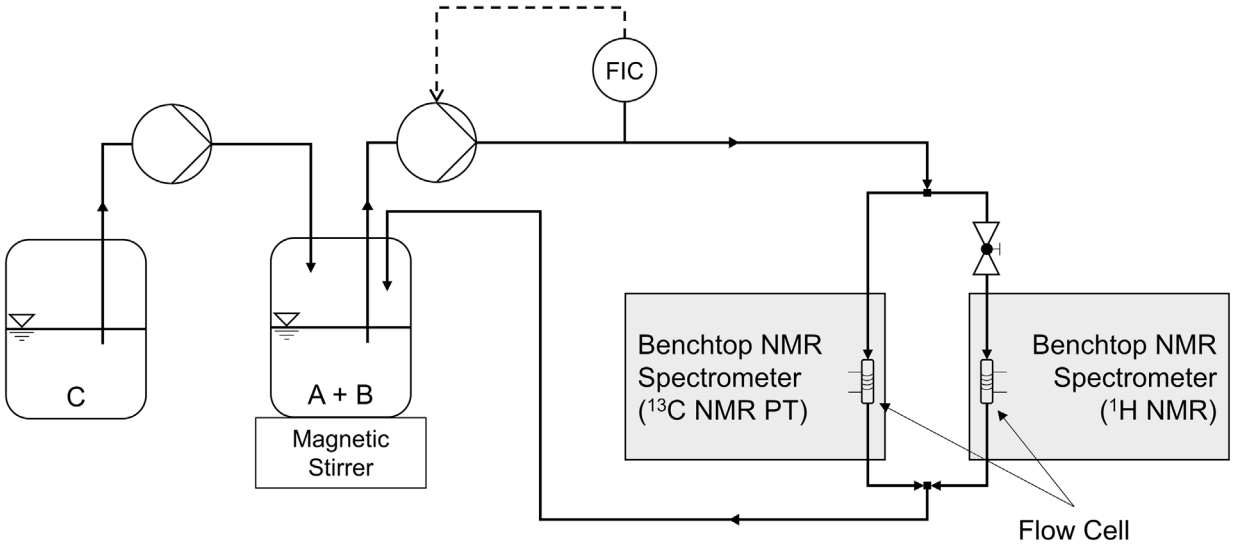

FIGURE 2 Scheme of the setup used for process monitoring experiments.

TABLE 2 Spin–lattice relaxation times $T_{1,^1H}$ and $T_{1,^{13}C}$ values of the CH_3-groups of each molecule in the studied ternary mixtures.

$T_{1,^1H}$ for System 1				$T_{1,^1H}$ for System 2			
	ACN	DMSO	EF		ACN	ACT	EF
Mixture	s			Mixture	s		
1.A	3.47 (28)	3.11 (3)	3.37 (2)	2.A	3.73 (4)	3.87 (2)	3.47 (1)
1.B	3.91 (2)	3.36 (2)	3.54 (3)	2.B	3.89 (4)	3.95 (13)	3.52 (16)
1.C	3.05 (5)	2.86 (3)	3.42 (5)	2.C	3.62 (4)	3.96 (1)	3.39 (3)
1.D	3.33 (1)	2.70 (1)	3.31 (1)	2.D	3.73 (2)	3.87 (3)	3.47 (1)
$T_{1,^{13}C}$ for System 1				$T_{1,^{13}C}$ for System 2			
	ACN	DMSO	EF		ACN	ACT	EF
Mixture	s			Mixture	s		
1.A	16.07	6.53	13.02	2.A	21.71	18.52	13.24
1.B	14.91	8.66	15.17	2.B	15.12	15.16	16.68
1.C	16.37	5.31	11.45	2.C	10.45	17.17	10.84
1.D	19.26	6.83	11.17	2.D	21.71	18.52	13.28

Note: The RMSE of three measurements is reported for $T_{1,^1H}$ in parentheses and refers to the last digit. For $T_{1,^{13}C}$, no RMSE is given as the measurement was done only once.

(A + B) was placed in the first container. A third component (C) was stored in the second container and was continuously fed by the second pump into the container with the mixture. Two dosage rates were used: $\dot{V} = 0.2$ mL min^{-1} and $\dot{V} = 0.833$ mL min^{-1}. The initial volume of the liquid mixture was about $V = 60$ mL. A magnetic stirrer (Topolino, IKA-Werke) was used to homogenize the mixture in the first container.

The setup includes two identical benchtop NMR spectrometers (Spinsolve Carbon, Magritek). The additional benchtop NMR spectrometer was also equipped with a glass flow cell (Spinsolve Reaction Monitoring Kit RM,

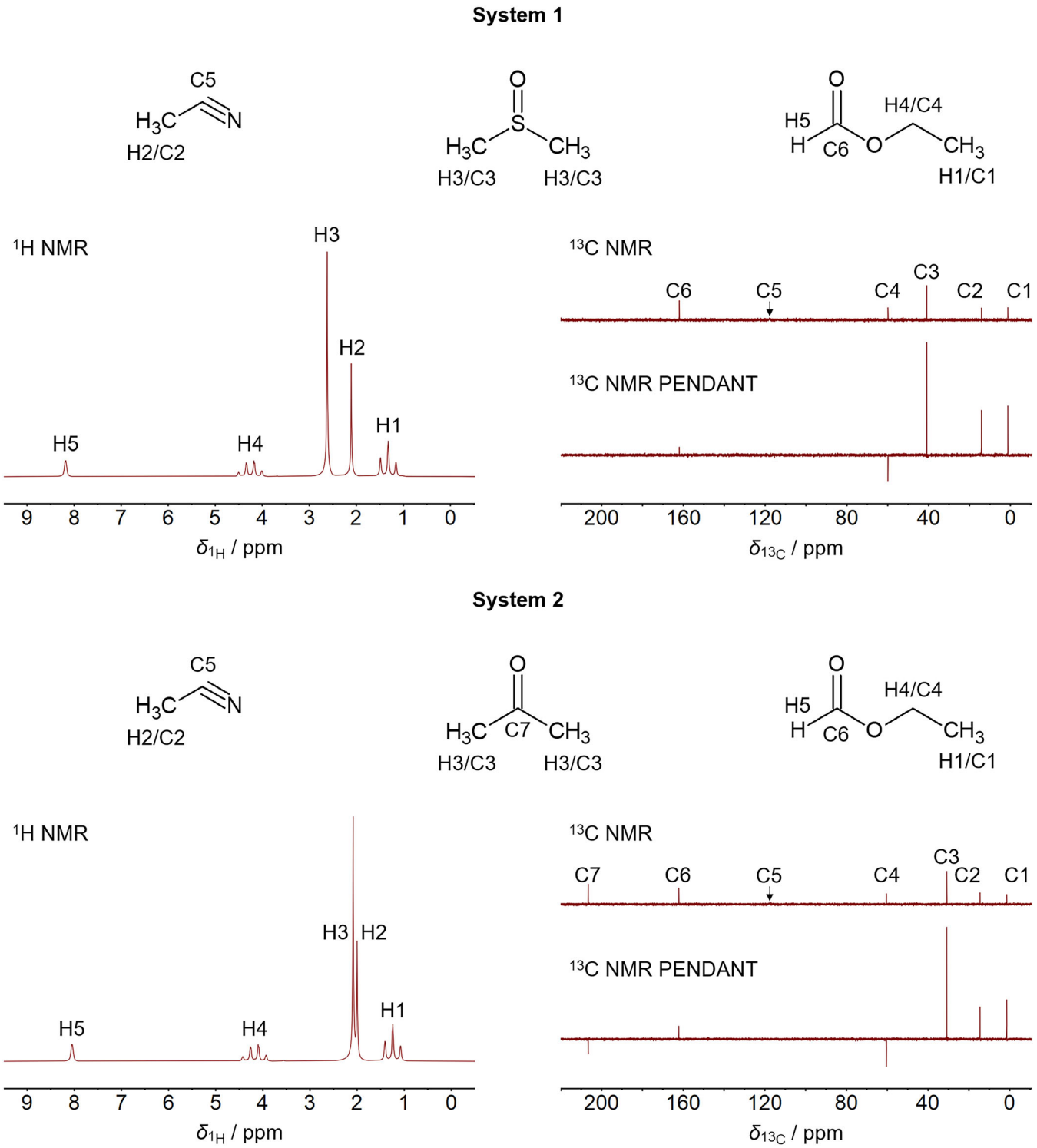

FIGURE 3 Comparison between ^{1}H NMR spectra as well as ^{13}C NMR and ^{13}C NMR PENDANT spectra for Mixture 1.A (top) and Mixture 2.A (bottom), respectively. PENDANT, polarization enhancement that is nurtured during attached nucleus testing.

Magritek) and was connected with PEEK capillaries with an inner diameter of $d = 1$ mm to the setup. T-pieces in combination with a needle valve were used to evenly distribute the volume flow of the sample mixture to the two benchtop NMR spectrometers. The pump that conveys the ternary mixture to the benchtop NMR spectrometers was set to a flow rate of $\dot{V} = 1.5$ mL min^{-1}. The first NMR spectrometer was used for ^{13}C NMR PENDANT experiments (3.2 s acquisition time, 16 k data points, 16 scans); the second NMR spectrometer was used for ^{1}H NMR experiments (6.4 s acquisition time, 32 k data points, 1 scan) for referencing purposes. Data were acquired with the second spectrometer in intervals of 15 s.

3 | RESULTS AND DISCUSSION

The $T_{1,^1H}$ and $T_{1,^{13}C}$ values of the CH_3-group of all components in the investigated mixtures are given in Table 2. In Figure 3, ^{1}H NMR as well as ^{13}C NMR and ^{13}C NMR PENDANT spectra are shown for Mixture 1.A and Mixture 2.A, respectively, including a peak assignment.

It can be seen from Figure 3 that the peaks in the ^{1}H NMR spectrum of Mixture 1.A are well-separated, which holds also for all other mixtures from ACN, DMSO, and EF. A quantification by direct peak integration can be carried out easily. In contrast, in Mixture 2.B, where DMSO is replaced by ACT, a peak overlap between the CH_3-groups of ACN and ACT occurs in the ^{1}H NMR spectrum. The components can no longer be quantified by direct peak integration and deconvolution methods must be applied.

In Figure 3, also ^{13}C NMR spectra of the studied mixtures are displayed together with the peak assignment. Due to the large chemical shift dispersion of ^{13}C, there is no peak overlap. However, the SNR of the ^{13}C NMR spectra is relatively low, despite the high number of 128 scans. The signal of the CN-group of ACN (C5) is barely visible at 120 ppm, which is attributed to the short spin–spin relaxation time T_2 of that group resulting in a broad signal. Furthermore, the total measurement time of more than 4 h for a single ^{13}C NMR spectrum is extremely long because of the long repetition time of five

TABLE 3 MAE and RMSE of the results from the quantification of the studied mixtures by ^{1}H NMR, ^{13}C NMR, and ^{13}C NMR PENDANT.

	System 1		System 2	
Experiment	**MAE**	**RMSE**	**MAE**	**RMSE**
^{1}H NMR	0.0059	0.0067	0.0201	0.0232
^{13}C NMR	0.0100	0.0127	0.0214	0.0261
^{13}C NMR PENDANT	0.0114	0.0153	0.0029	0.0038

Abbreviations: MAE, mean absolute error; PENDANT, polarization enhancement that is nurtured during attached nucleus testing; RMSE, root mean squared error.

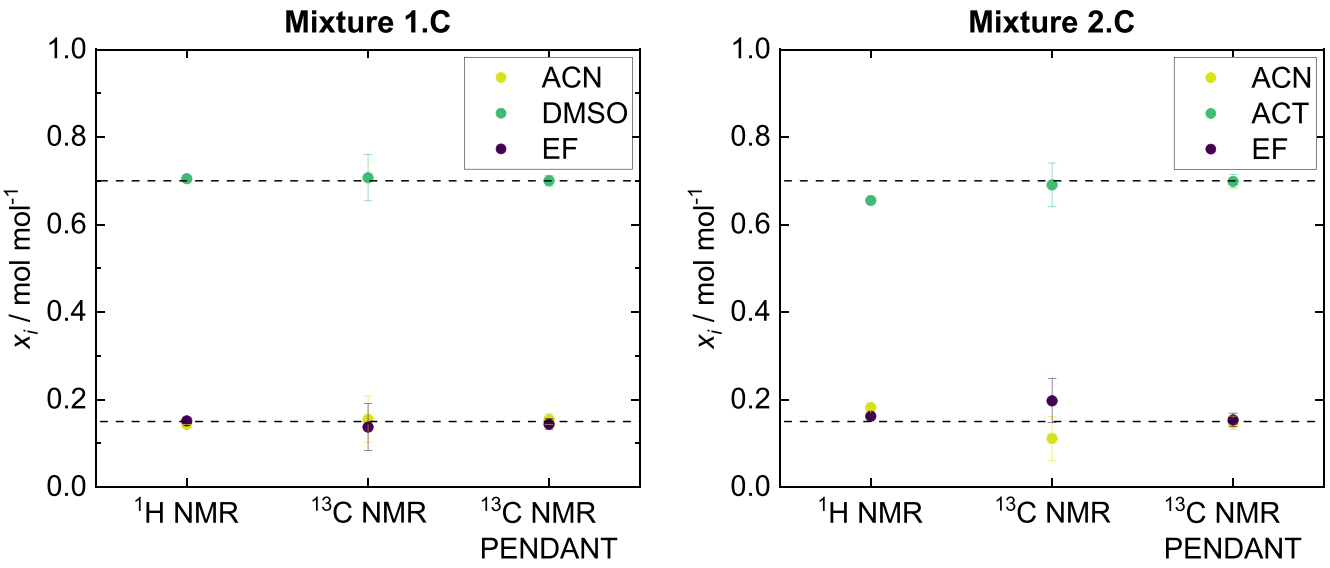

FIGURE 4 Results for the quantification of Mixture 1.C and Mixture 2.C by ^{1}H NMR, ^{13}C NMR, and ^{13}C NMR PENDANT experiments. The horizontal dashed lines are results from the gravimetric sample preparation. The uncertainties (error bars) for the ^{1}H NMR experiments are within the symbol size. The concentrations of ACN and EF were equal in both cases. PENDANT, polarization enhancement that is nurtured during attached nucleus testing.

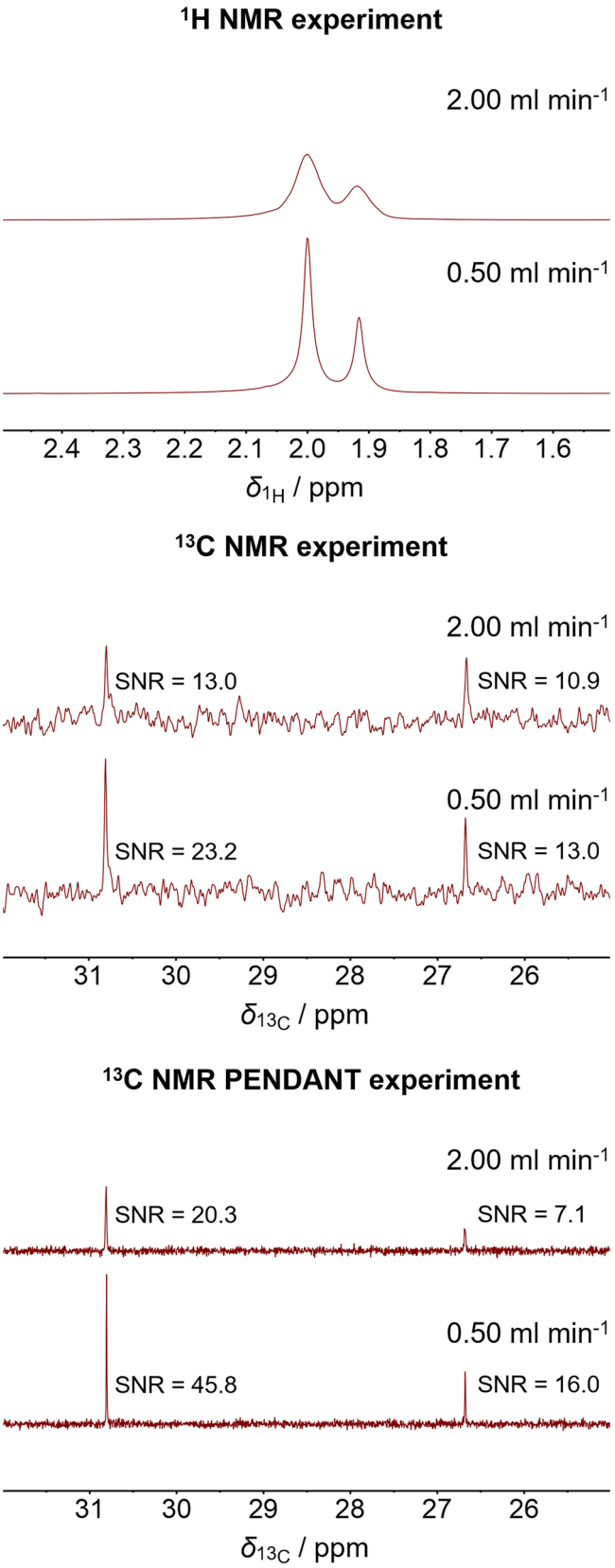

FIGURE 5 Spectra of the Mixture 2.A acquired with ^{1}H NMR, ^{13}C NMR and ^{13}C NMR PENDANT experiments at two different flow rates. The peaks of ACN and ACT are shown. The SNRs are given for the ^{13}C NMR and ^{13}C NMR PENDANT spectra. PENDANT, polarization enhancement that is nurtured during attached nucleus testing. PENDANT, polarization enhancement that is nurtured during attached nucleus testing; SNR, signal-to-noise ratio.

times $T_{1,^{13}C}$ required for full magnetization recovery, which is necessary for a quantitative measurement. For use in process monitoring under continuous flow, this is not practical.

Figure 3 also shows results from experiments that were carried out using ^{13}C NMR PENDANT. The settings were chosen so that the full enhancement is obtained for the signals from CH_3-groups, as only these were used for the quantification. The sequence could have been adjusted to enhance signals from CH_2- and CH-group likewise. For the CH_3-groups, an enhancement of the SNR of about 3.5 was obtained; see signals C1–C3 in Figure 3. We note that a signal from the quaternary C atom in ACT is obtained with PENDANT (however, as expected without enhancement). This is not the case for other polarization transfer sequences, such as INEPT and DEPT.

Another advantageous feature of PENDANT (and other polarization transfer methods such as DEPT) is its selectivity for different functional groups: signals from CH_2-groups as well as from quaternary C atoms are negative, while those from CH_3- and CH-groups are positive; see Figure 3. This is useful for the identification of components in complex mixtures.

Another important advantage of polarization transfer is that for the recycle delay, not the high $T_{1,^{13}C}$ is relevant, but the much lower $T_{1,^{1}H}$. Therefore, in the experiment shown in Figure 3, which both had 128 scans, the total experimental time for the ^{13}C NMR PENDANT experiment was reduced by a factor of 5 compared with the ^{13}C NMR experiment. In the following sections, we study whether ^{13}C NMR PENDANT yields quantitative results in stationary as well as in flow experiments.

3.1 | Stationary experiments

Figure 4 shows results from the quantitative analysis of System 1 and System 2 with conventional ^{1}H NMR and ^{13}C NMR as well as ^{13}C NMR PENDANT experiments. For comparison, also the results from the gravimetric sample preparation are shown that are considered here as the ground truth and are depicted as horizontal dashed lines. Figure 4 shows the results for Mixture 1.C and Mixture 2.C; the corresponding results for the other mixtures are shown in the Supporting Information. The MAE and RMSE values of the quantification results of the analyzed mixtures are presented in Table 3. The numerical results of all experiments are provided in the Supporting Information (Table SI. 3).

Figure 4 shows that results from all three methods are generally in good agreement with the gravimetric reference, which also holds for the other studied mixtures. A closer inspection, however, reveals some differences (also see Table SI. 3 which contains the numerical results in the Supporting Information): Firstly, the experimental uncertainty is generally much lower for ^{13}C NMR PENDANT compared with ^{13}C NMR. However, it is always higher than for ^{1}H NMR in System 1, which is a result of the fact that they are calculated from the SNR. Secondly, the results for all methods are quite good for System 1 with values for the MAE and RMSE of about 0.011 and 0.015, respectively. However, for System 2, which is analytically more demanding, the results from ^{13}C NMR PENDANT are better than for ^{1}H NMR and have even smaller errors than the ones obtained for System 1; see MAE (0.003) and RMSE (0.004). In contrast, the error values for ^{1}H NMR and ^{13}C NMR are distinctly higher. The larger deviation for the ^{1}H NMR method is due to difficulties in the deconvolution of the overlapping peaks. Moreover, in comparing the ^{13}C NMR results to the ^{13}C NMR PENDANT results, it has to be considered that the latter were obtained in experiments that were about 5 times faster.

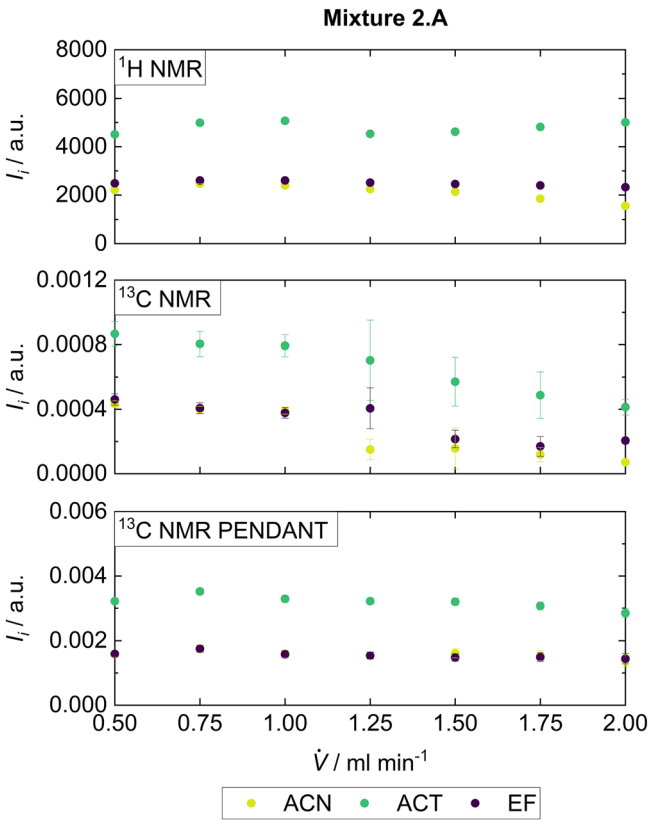

FIGURE 6 Peak integrals of the CH_3-groups of ACN, ACT and EF in Mixture 2.A acquired with ^{1}H NMR, ^{13}C NMR and ^{13}C NMR PENDANT experiments at various flow rates. The error bars are calculated by the SNR of the peak. PENDANT, polarization enhancement that is nurtured during attached nucleus testing; SNR, signal-to-noise ratio.

3.2 | Flow experiments

All test mixtures were analyzed with ^{1}H NMR, ^{13}C NMR and ^{13}C NMR PENDANT in flow experiments with different flow rates. The flow rate has an effect on the peak width determined by the spin-spin relaxation time T_2^*, and on the build-up of magnetization of the spins determined by the spin–lattice relaxation time T_1.[3,10] The effect of increasing flow rates on the ^{1}H NMR, ^{13}C NMR and ^{13}C NMR PENDANT spectra is shown in Figure 5, using Mixture 2.A as an example.

In the ^{1}H NMR spectra, the SNR is consistently high at all flow rates. However, the ^{13}C NMR spectra display a very low SNR which decreases at higher flow rates. In contrast, the ^{13}C NMR PENDANT spectra show a significantly higher SNR. Furthermore, it can be observed for all experiments that the peak heights decline at higher flow rates while the linewidths increase. This is due to the shortening of the spin-spin relaxation time T_2^* and the reduction of the premagnetization time. The peak broadening is especially disadvantageous in the ^{1}H NMR spectra as it may result in an increased peak overlap, as it can be seen in the ^{1}H NMR spectra near 2 ppm: the signals of the CH_3-groups of ACN and ACT strongly overlap at high flow rates which causes problems in the quantitative analysis.

The effect of the shorter premagnetization time at higher flow rates on the peak integrals acquired by ^{1}H NMR, ^{13}C NMR and ^{13}C NMR PENDANT experiments is illustrated in Figure 6, using again Mixture 2.A as an example. In all experiments the peak integrals decrease with higher flow rates. However, the decrease is particularly critical for the ^{13}C NMR experiment because of the large $T_{1,^{13}C}$ values. In addition, there are significant differences between the $T_{1,^{13}C}$ values of the different components (see Table 2) causing an uneven magnetization and, hence, deviations in the quantification. In the ^{13}C NMR PENDANT experiment, the premagnetization is sufficient throughout and the signal decrease is equal between each component at all flow rates (a signal drop of 10 % at $\dot{V} = 2.0$ mL min^{-1} for each component), since the used $T_{1,^{1}H}$ values are small and in a similar range, which allows quantitative analysis.

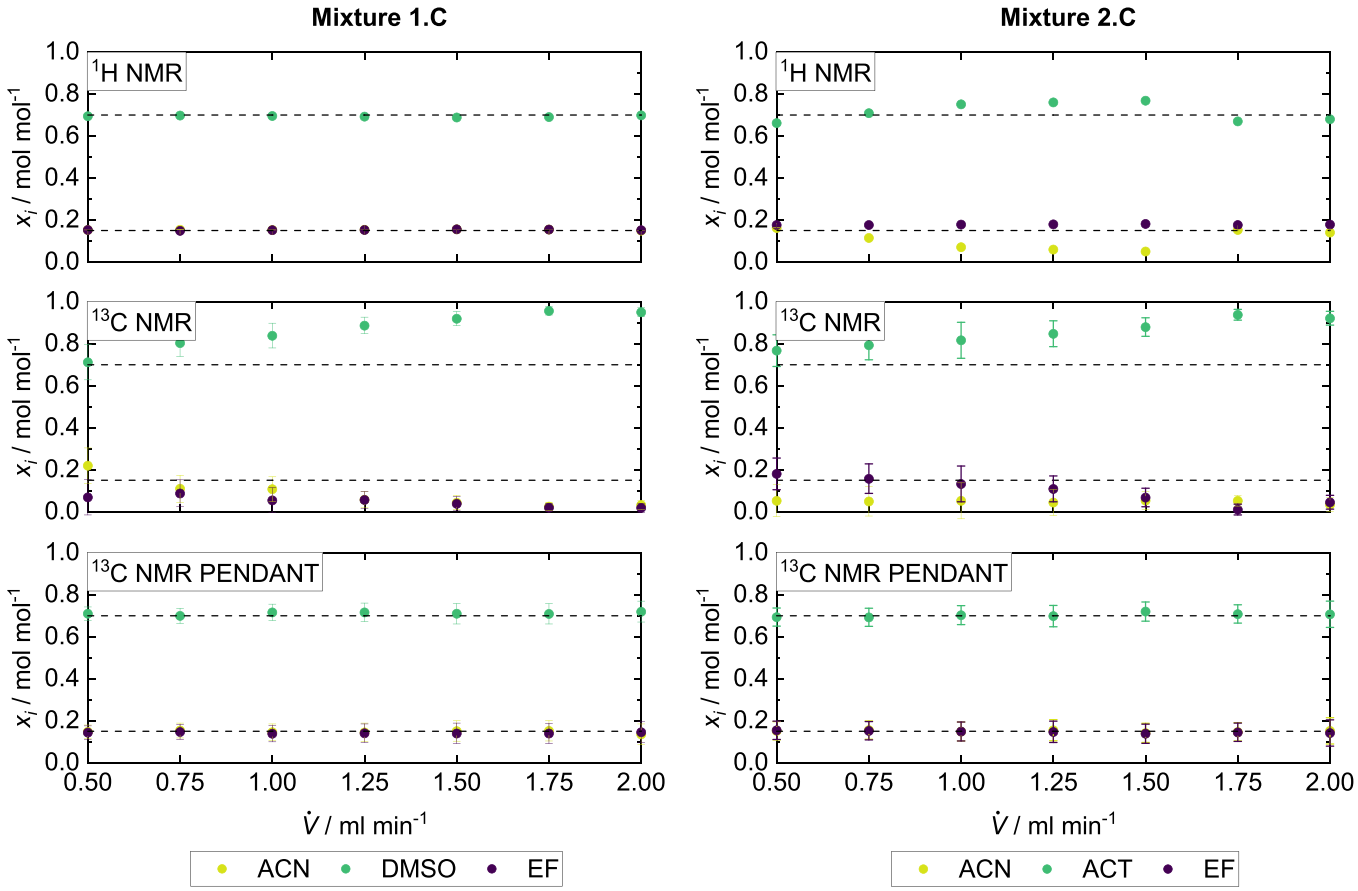

FIGURE 7 Results of the quantitative analysis of Mixture 1.C and Mixture 2.C by ^{1}H NMR, ^{13}C NMR and ^{13}C NMR PENDANT in flow experiments at different flow rates. The horizontal dashed lines represent the gravimetric reference. The error bars for the ^{1}H NMR experiments are within the symbol size. PENDANT, polarization enhancement that is nurtured during attached nucleus testing.

In the following, the influence of the flow effects on the quantification of the mixtures with ^{1}H NMR, ^{13}C NMR and ^{13}C NMR PENDANT experiments is discussed. In Figure 7 the results obtained in studies of the Mixture 1.C and Mixture 2.C at various flow rates are shown. The reference values are depicted as dashed horizontal lines. Similar representations of the results for the other mixtures as well as the numerical results are given in the Supporting Information.

As shown in Figure 7 for System 1, the concentrations obtained by the ^{1}H NMR experiment are in very good agreement with the gravimetric reference, even at the highest flow rates. It is noteworthy that this agreement was obtained despite the fact that no full magnetization was achieved at high flow rates (for a calculation of the magnetization, see Supporting Information). This is due to the fact that the $T_{1,^{1}\mathrm{H}}$ values for all components are very similar and hence the premagnetization is very similar. Furthermore, the error bars are small due to the high SNR of the ^{1}H 0NMR experiment resulting in an accurate quantification.

The results from the ^{13}C NMR experiments deviate strongly from the gravimetric reference even at moderate flow rates. The concentration of DMSO is overestimated, those of ACN and EF are underestimated, with deviations that tend to increase with increasing flow rate. This observation can be explained by large differences in the spin–lattice relaxation times $T_{1,^{13}\mathrm{C}}$ of the components (see Table 2). The negative effect of insufficient premagnetization of ACN and EF is amplified at high flow rates. The small SNR in the ^{13}C NMR spectrum leads to additional problems with the quantification resulting, for example, in large error bars.

In contrast, the ^{13}C NMR PENDANT experiment shows very good agreement with the gravimetric reference, also at the highest flow rates; see Figure 7. In addition, the error bars of the ^{13}C NMR PENDANT experiments are small compared with the ^{13}C NMR experiment due to the signal enhancement, which leads to higher SNR.

For System 2, the results from the ^{1}H NMR flow experiments deviate from the gravimetric reference, as it was the case in the stationary experiments. However, the deviations show no clear dependency on the flow rate. While the results for the concentration of EF are fair for all flow rates, there are important deviations for ACN and ACT, due to the strongly overlapping peaks. For Mixture 2.C, even a fusion of both singlets was observed which is challenging for the deconvolution and results in incorrect concentrations.

The results of the ^{13}C NMR experiments for System 1 and System 2 show similar and important deviations from the gravimetric reference. In contrast, the results obtained by ^{13}C NMR PENDANT are in very good agreement with the reference. The reasons for this excellent performance are the same as already discussed for System 1. In System 2, however, the advantage of the ^{13}C NMR PENDANT experiment is more pronounced, as peak overlap problems occur in this system in the ^{1}H NMR experiments.

3.3 | Process monitoring experiments

A continuous dilution experiment to mimic a dynamic process was performed with the setup shown in Figure 2 which enables the simultaneous acquisition of

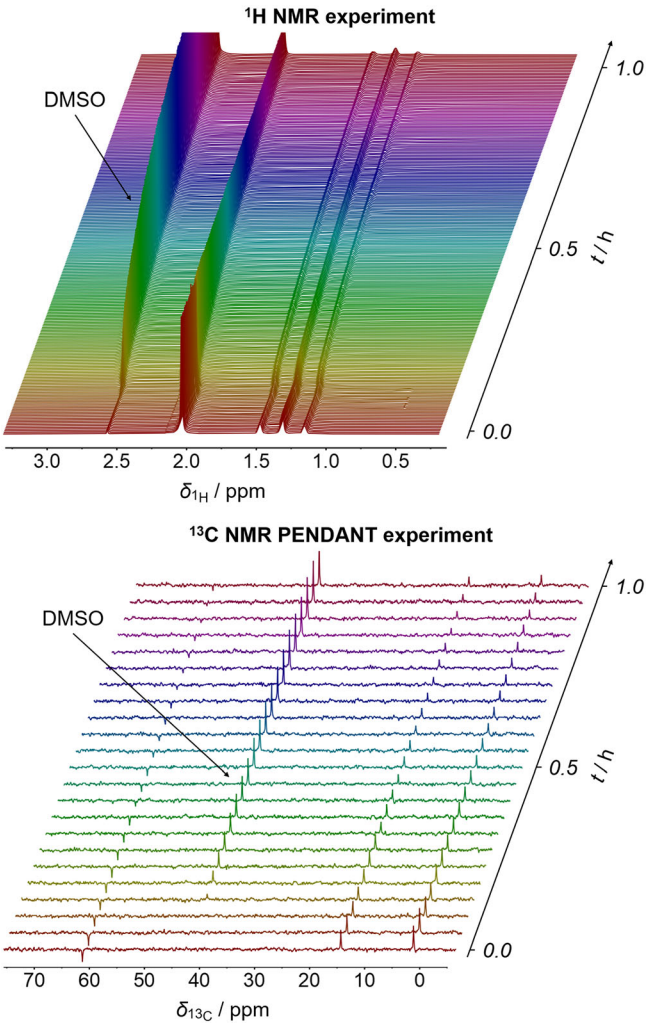

FIGURE 8 Monitoring of a dilution experiment in System 1 with ^{1}H NMR and ^{13}C NMR PENDANT experiments. DMSO was continuously added to a binary mixture of ACN + EF (initial concentration $x_{\mathrm{ACN}} = 0.6$ mol mol^{-1}) within a time interval of 1 h (corresponding to a dosage rate of $\dot{V} = 0.833$ mL min^{-1}). PENDANT, polarization enhancement that is nurtured during attached nucleus testing.

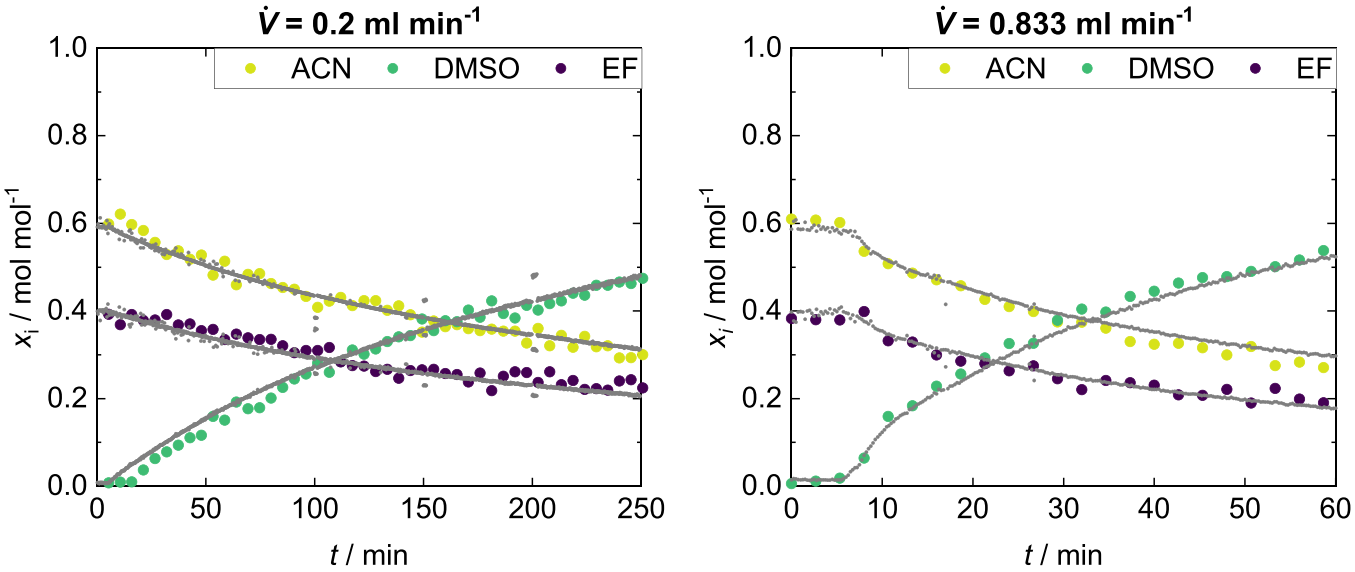

FIGURE 9 Results of the quantitative analysis of System 1 with ^{1}H NMR and ^{13}C NMR PENDANT during the monitoring of a continuous dilution experiment. DMSO was continuously added to a binary mixture of ACN + EF (initial concentration $x_{ACN} = 0.6$ mol mol^{-1}) within 4 h (dosage rate: $\dot{V} = 0.2$ mL min^{-1}, left) and 1 h (dosage rate: $\dot{V} = 0.833$ mL min^{-1}, right), respectively. The gray circles (appearing as gray lines due to the high acquisition rate) represent the concentrations determined by ^{1}H NMR. The colored circles are from ^{13}C NMR PENDANT. The error bars are not shown for clarity. PENDANT, polarization enhancement that is nurtured during attached nucleus testing.

^{1}H NMR and ^{13}C NMR PENDANT spectra. System 1 was used for this study which allows to consider the results of ^{1}H NMR experiments as reference as there is no peak overlap in the ^{1}H NMR spectrum. Furthermore, the effect of two dosage rates on the quality of the determined concentrations by the ^{13}C NMR PENDANT experiment was investigated. In both cases, DMSO was continuously added to a mixture of ACN + EF with an initial concentration of $x_{ACN} = 0.6$ mol mol^{-1}. In the first experiment a DMSO dosage rate of $\dot{V} = 0.2$ mL min^{-1} was used, resulting in a total study time of 4 h. In the second experiment, the dosage rate was increased to $\dot{V} = 0.833$ mL min^{-1}, which reduces the study time to 1 h. The ^{1}H NMR and ^{13}C NMR PENDANT spectra from the second experiment are shown in Figure 8. The effective flow rate in each spectrometer was $\dot{V} = 0.75$ mL min^{-1}.

Figure 8 shows that the NMR signal of DMSO continuously increases in the ^{1}H NMR as well as in the ^{13}C NMR PENDANT spectra during the progress of the dilution experiment. The ^{1}H NMR experiment has a high temporal resolution because only one scan is required for the quantitative analysis as the SNR in the ^{1}H NMR spectra is sufficiently high. The ^{13}C NMR PENDANT experiment requires 16 scans to obtain a sufficient SNR for the quantification resulting in a measurement time of 2.7 min so that 24 ^{13}C NMR PENDANT spectra were taken in the course of the experiment. The results of the quantitative analysis of both dilution experiments are shown in Figure 9.

For both experiments, there is a time lag of about 5 min, until the concentration change can be observed, which is, however, better visible in the results for the high dosage rate. As could be expected, the concentration changes, resulting from the addition of DMSO with a constant flow rate, are not linear. The concentrations determined with ^{13}C NMR PENDANT are in very good agreement with those from ^{1}H NMR. The scattering of the results from ^{13}C NMR PENDANT is about 0.04 mol mol^{-1}, which is a consequence of the low number of 16 scans that was used, but a smoothing of the results obtained at different times would obviously lead to a result that is very close to the ^{1}H NMR reference. Similar results from ^{13}C NMR PENDANT could be expected for System 2, for which, however, ^{1}H NMR would have given only poor results due to the peak overlap (see Section 3.2), and ^{13}C NMR could not be reasonably used with only 16 scans due to the low SNR.

4 | CONCLUSIONS

In this work, we have applied the polarization transfer sequence PENDANT for the quantitative analysis of mixtures in stationary and flow experiments with a

benchtop NMR spectrometer. The new method combines three advantages: fast premagnetization, high spectral resolution, and good SNR. The accuracy and reliability of quantitative results obtained with ^{13}C NMR PENDANT were evaluated and compared with results from ^{1}H NMR, ^{13}C NMR, and a gravimetric reference. It was shown that ^{13}C NMR PENDANT gives excellent results also at conditions where ^{13}C NMR without polarization transfer cannot be applied, for example, in measurements at high flow rates that cause problems in the analysis with benchtop NMR spectrometers, due to their low premagnetization volume. The new method is particularly attractive for the analysis of mixtures that are difficult to quantify with ^{1}H NMR due to overlapping peaks. Furthermore, we have also demonstrated that the ^{13}C NMR PENDANT is useful for monitoring dynamic processes. Future investigations will focus on the combination of this method with hyperpolarization techniques, such as Overhauser dynamic nuclear polarization, in order to obtain further signal enhancements.

ACKNOWLEDGMENTS

The authors thank the German Research Foundation (DFG) for the financial support within the Collaborative Research Center SFB 1527 HyPERiON. The authors thank Andreas Müller for his contribution to the experiments of this work.

ORCID

Johnnie Phuong https://orcid.org/0009-0004-3878-0230
Hans Hasse https://orcid.org/0000-0003-4612-5995
Kerstin Münnemann https://orcid.org/0000-0001-5247-8856

REFERENCES

[1] R. Hotop, *Chem. Ing. Tech.* **1993**, *65*(8), 921. https://doi.org/10.1002/cite.330650805
[2] A. Brächer, R. Behrens, E. von Harbou, H. Hasse, *Chem. Eng. J.* **2016**, *306*, 413. https://doi.org/10.1016/j.cej.2016.07.045
[3] A. M. R. Hall, J. C. Chouler, A. Codina, P. T. Gierth, J. P. Lowe, U. Hintermair, *Catal. Sci. Technol.* **2016**, *6*(24), 8406. https://doi.org/10.1039/c6cy01754a
[4] M. Maiwald, H. H. Fischer, Y.-K. Kim, K. Albert, H. Hasse, *J. Magn. Reson.* **2004**, *166*(2), 135. https://doi.org/10.1016/j.jmr.2003.09.003
[5] M. Maiwald, H. H. Fischer, Y.-K. Kim, H. Hasse, *Anal. Bioanal. Chem.* **2003**, *375*(8), 1111. https://doi.org/10.1007/s00216-002-1723-y
[6] A. Nordon, C. A. McGill, D. Littlejohn, *Analyst* **2001**, *126*(2), 260. https://doi.org/10.1039/b009293m
[7] E. von Harbou, R. Behrens, J. Berje, A. Brächer, H. Hasse, *Chem. Ing. Tech.* **2016**, *89*(4), 369. https://doi.org/10.1002/cite.201600068
[8] N. Zientek, K. Meyer, S. Kern, M. Maiwald, *Chem. Ing. Tech.* **2016**, *88*(6), 698. https://doi.org/10.1002/cite.201500120
[9] B. Blümich, *TrAC Trends Anal. Chem.* **2016**, *83*, 2. https://doi.org/10.1016/j.trac.2015.12.012
[10] F. Dalitz, M. Cudaj, M. Maiwald, G. Guthausen, *Prog. Nucl. Magn. Reson. Spectrosc.* **2012**, *60*, 52. https://doi.org/10.1016/j.pnmrs.2011.11.003
[11] E. Danieli, J. Perlo, A. L. L. Duchateau, G. K. M. Verzijl, V. M. Litvinov, B. Blümich, F. Casanova, *ChemPhysChem* **2014**, *15*(14), 3060. https://doi.org/10.1002/cphc.201402049
[12] M. V. S. Elipe, R. R. Milburn, *Magn. Reson. Chem.* **2015**, *54*(6), 437. https://doi.org/10.1002/mrc.4189
[13] M. Grootveld, B. Percival, M. Gibson, Y. Osman, M. Edgar, M. Molinari, M. L. Mather, F. Casanova, P. B. Wilson, *Anal. Chim. Acta* **2019**, *1067*, 11. https://doi.org/10.1016/j.aca.2019.02.026
[14] T. Maschmeyer, P. L. Prieto, S. Grunert, J. E. Hein, *Magn. Reson. Chem.* **2020**, *58*(12), 1234. https://doi.org/10.1002/mrc.5094
[15] K. Meyer, S. Kern, N. Zientek, G. Guthausen, M. Maiwald, *TrAC Trends Anal. Chem.* **2016**, *83*, 39. https://doi.org/10.1016/j.trac.2016.03.016
[16] T. Rudszuck, H. Nirschl, G. Guthausen, *J. Magn. Reson.* **2021**, *323*, 106897. https://doi.org/10.1016/j.jmr.2020.106897
[17] K. Singh, B. Blümich, *TrAC Trends Anal. Chem.* **2016**, *83*, 12. https://doi.org/10.1016/j.trac.2016.02.014
[18] T. A. Beek, *Phytochem. Anal.* **2020**, *32*(1), 24. https://doi.org/10.1002/pca.2921
[19] D. Bouillaud, J. Farjon, O. Gonçalves, P. Giraudeau, *Magn. Reson. Chem.* **2019**, *57*(10), 794. https://doi.org/10.1002/mrc.4821
[20] T. Castaing-Cordier, D. Bouillaud, J. Farjon, P. Giraudeau, *Annu. Rep. NMR Spectrosc.* **2021**, *103*, 191. https://doi.org/10.1016/bs.arnmr.2021.02.003
[21] C. Claaßen, K. Mack, D. Rother, *ChemCatChem* **2020**, *12*(4), 1190. https://doi.org/10.1002/cctc.201901910
[22] F. Dalitz, L. Kreckel, M. Maiwald, G. Guthausen, *Appl. Magn. Reson.* **2014**, *45*(5), 411. https://doi.org/10.1007/s00723-014-0522-x
[23] A. Friebel, E. von Harbou, K. Münnemann, H. Hasse, *Indust. Eng. Chem. Res.* **2019**, *58*(39), 18125. https://doi.org/10.1021/acs.iecr.9b03048
[24] A. Friebel, E. von Harbou, K. Münnemann, H. Hasse, *Chem. Eng. Sci.* **2020**, *219*, 115561. https://doi.org/10.1016/j.ces.2020.115561
[25] D. Galvan, L. M. de Aguiar, J. J. R. Rohwedder, D. Borsato, M. H. M. Killner, *Fuel Process. Technol.* **2020**, *208*, 106511. https://doi.org/10.1016/j.fuproc.2020.106511
[26] S. Kern, S. Liehr, L. Wander, M. Bornemann-Pfeiffer, S. Müller, M. Maiwald, S. Kowarik, *Anal. Bioanal. Chem.* **2020**, *412*(18), 4447. https://doi.org/10.1007/s00216-020-02687-5
[27] S. Kern, L. Wander, K. Meyer, S. Guhl, A. R. G. Mukkula, M. Holtkamp, M. Salge, C. Fleischer, N. Weber, R. King, S. Engell, A. Paul, M. P. Remelhe, M. Maiwald, *Anal. Bioanal. Chem.* **2019**, *411*(14), 3037. https://doi.org/10.1007/s00216-019-01752-y
[28] D. Kreyenschulte, E. Paciok, L. Regestein, B. Blümich, J. Büchs, *Biotechnol. Bioeng.* **2015**, *112*(9), 1810. https://doi.org/10.1002/bit.25599

[29] A. Soyler, D. Bouillaud, J. Farjon, P. Giraudeau, M. H. Oztop, *LWT* **2020**, *118*, 108832. https://doi.org/10.1016/j.lwt.2019.108832
[30] Y. Matviychuk, E. Steimers, E. von Harbou, D. J. Holland, *J. Magn. Reson.* **2020**, *319*, 106814. https://doi.org/10.1016/j.jmr.2020.106814
[31] Y. Matviychuk, E. von Harbou, D. J. Holland, *J. Magn. Reson.* **2017**, *285*, 86. https://doi.org/10.1016/j.jmr.2017.10.009
[32] Y. Matviychuk, J. Yeo, D. J. Holland, *J. Magn. Reson.* **2019**, *298*, 35. https://doi.org/10.1016/j.jmr.2018.11.010
[33] E. Steimers, Y. Matviychuk, A. Friebel, K. Münnemann, E. Harbou, D. J. Holland, *Magn. Reson. Chem.* **2020**, *59*(3), 221. https://doi.org/10.1002/mrc.5095
[34] B. Gouilleux, B. Charrier, S. Akoka, F.-X. Felpin, M. Rodriguez-Zubiri, P. Giraudeau, *TrAC Trends Anal. Chem.* **2016**, *83*, 65. https://doi.org/10.1016/j.trac.2016.01.014
[35] B. Gouilleux, B. Charrier, E. Danieli, J.-N. Dumez, S. Akoka, F.-X. Felpin, M. Rodriguez-Zubiri, P. Giraudeau, *Analyst* **2015**, *140*(23), 7854. https://doi.org/10.1039/c5an01998b
[36] X. Li, K. Hu, *Annu. Rep. NMR Spectrosc.* **2017**, 90, 85. https://doi.org/10.1016/bs.arnmr.2016.08.001
[37] D. A. L. Otte, D. E. Borchmann, C. Lin, M. Weck, K. A. Woerpel, *Org. Lett.* **2014**, *16*(6), 1566. https://doi.org/10.1021/ol403776k
[38] J. van Duynhoven, E. van Velzen, D. M. Jacobs, *Annu. Rep. NMR Spectrosc.* **2013**, *80*, 181. https://doi.org/10.1016/b978-0-12-408097-3.00003-2
[39] A. Friebel, T. Specht, E. von Harbou, K. Münnemann, H. Hasse, *J. Magn. Reson.* **2020**, *312*, 106683. https://doi.org/10.1016/j.jmr.2020.106683
[40] H. H. Fischer, M. Seiler, T. S. Ertl, U. Eberhardinger, H. Bertagnolli, H. Schmitt-Willich, K. Albert, *J. Phys. Chem. B* **2003**, *107*(20), 4879. https://doi.org/10.1021/jp021631d
[41] K. Albert, M. Nieder, E. Bayer, M. Spraul, *J. Chromatogr. A* **1985**, *346*, 17. https://doi.org/10.1016/s0021-9673(00)90489-8
[42] T. J. Henderson, *J. Am. Chem. Soc.* **2004**, *126*(12), 3682. https://doi.org/10.1021/ja039261+
[43] A. V. Mäkelä, I. Kilpeläinen, S. Heikkinen, *J. Magn. Reson.* **2010**, *204*(1), 124. https://doi.org/10.1016/j.jmr.2010.02.015
[44] J. Homer, M. C. Perry, *J. Chem. Soc. Chem. Commun.* **1994**, *4*, 373. https://doi.org/10.1039/c39940000373
[45] J. Homer, M. C. Perry, *J. Chem. Soc. Perkin Trans.* **1995**, *2*(3), 533. https://doi.org/10.1039/p29950000533
[46] M. Sawall, E. von Harbou, A. Moog, R. Behrens, H. Schröder, J. Simoneau, E. Steimers, K. Neymeyr, *J. Magn. Reson.* **2018**, *289*, 132. https://doi.org/10.1016/j.jmr.2018.02.012
[47] E. Steimers, M. Sawall, R. Behrens, D. Meinhardt, J. Simoneau, K. Münnemann, K. Neymeyr, E. von Harbou, *Magn. Reson. Chem.* **2020**, *58*(3), 260. https://doi.org/10.1002/mrc.4964

SUPPORTING INFORMATION

Additional supporting information can be found online in the Supporting Information section at the end of this article.

How to cite this article: J. Phuong, Z. Romero, H. Hasse, K. Münnemann, *Magn Reson Chem* **2024**, *62*(5), 398. https://doi.org/10.1002/mrc.5417